

COMMISSIONING OF UNIVERSAL SPLIT HOPKINSON BAR FOR DYNAMIC COMPRESSION AND TENSION EXPERIMENTS

LUKÁŠ KOCIAN*, JAN FALTA, NELA KRČMÁŘOVÁ, TOMÁŠ FÍLA,
JAN ŠLEICHRT

*Czech Technical University in Prague, Faculty of Transportational Sciences, Na Florenci 1324/25, 110 00
Prague – Nové Město, Czech Republic*

* corresponding author: kocialuk@cvut.cz

ABSTRACT. Split Hopkinson Bar is an experimental apparatus designed for acquiring material properties in dynamic regime. The apparatus is usually constructed as a single purpose experimental device for specific type of loading, most commonly either compression (Split Hopkinson Pressure Bar) or tension (Split Hopkinson Tensile Bar). In this paper, a simple and highly modular design capable of testing for multiple types of loading is introduced, which can be a great advantage to obtain material properties under different loading conditions. The device was successfully assembled, including its electrical installation and implementation of a pneumatic launching system and was fitted with multiple sensors. Series of calibration procedures was conducted successfully to analyze correct behaviour of the system. After calibration, the apparatus was subjected to multiple pilot tests with samples manufactured using 3D printing. The results were compared to those obtained using the quasi-static method.

KEYWORDS: Split Hopkinson Bar, dynamic tension and compression, experimental impact dynamics, additive manufacturing, high strain-rate testing.

1. INTRODUCTION

High strain-rate testing plays a vital role in determining the behavior and mechanical properties of materials subjected to dynamic loads occurring for instance in collisions of moving objects such as cars or trains and represents current trend for material testing under relevant conditions. Knowing the material behaviour under dynamic loading has its use in numerical constitutive modeling that helps to predict outcomes of impact events such as traffic accidents or in defense industry. One of the most common testing devices used for dynamic experiments is the Split Hopkinson Bar (SHB) which is commonly designed as a single purpose apparatus with a design tailored for a certain application, e.g., compression or tensile testing. The device follows the principles pioneered in the works of Kolsky [1], Davies [2] and Krafft [3]. It uses an impact of a striker accelerated commonly using a pneumatic launching system and the material properties are evaluated by capturing strain data of waves propagating through two bars with a sample placed between them. This classical arrangement of the experimental setup is well established for testing of conventional materials such metals and alloys particularly in uni-axial compression. However, many variants were derived from this classical arrangement over time to serve better in a specific application. Specialized setups for testing of materials under specific dynamic conditions, e.g, shear [4], large deformation of sheet metals [5], interlaminar delamination [6], or large deformation of lattice structures [7] have been developed and suc-

cessfully used. A specific topic is testing under direct impact conditions using instrumented apparatus [8–10] that is particularly favourable in dynamic analysis of cellular solids [11–13]. While the testing apparatuses are usually designed on purpose for a specific application requiring modifications of the experimental setup, it is beneficial to design an apparatus with an extensive modularity, versatility and flexibility allowing for easy re-assembly and testing under different loading conditions. In this paper, a highly modular modification of standard design with a capability for both uni-axial types of loading (tension and compression), as well as direct impact testing and experiments with multiple bar arrangements is introduced. The device is aptly named Universal Split Hopkinson Bar (USHB) and its design, commissioning, calibration and pilot measurements are described and discussed in the paper.

2. MATERIALS AND METHODS

2.1. UNIVERSAL SPLIT HOPKINSON BAR

USHB was designed as a highly modular system allowing for experiments in uni-axial compression and tension while it even supports more complex arrangements, for instance two parallel output bars. No excessive re-assembly is necessary to switch tests from compression to tension and vice versa. Bearing supports are constructed in a way to provide easy alignment, installation and removal of the individual bars without affecting rest of the system. To keep the costs low and the design as simple as possible, the bar system has

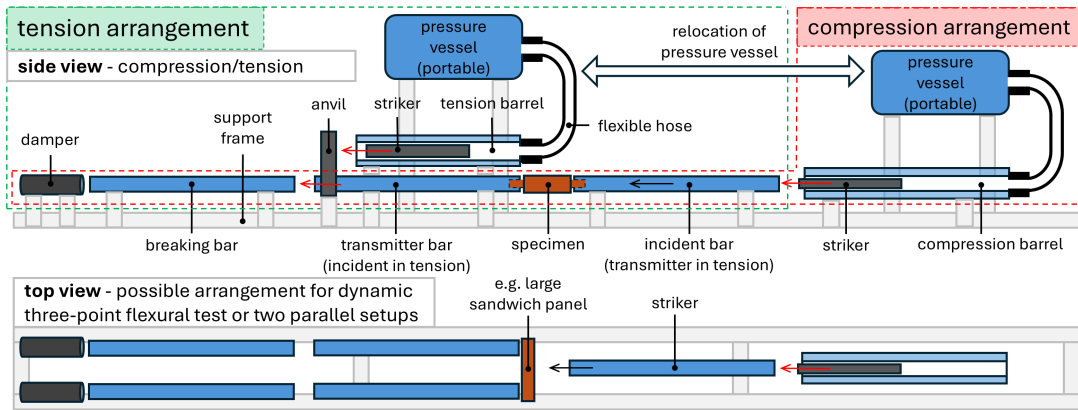


FIGURE 1. A full schematic of USHB.

two gas-gun barrels (one for tensile testing and other one for compression testing) while the compressed air launching system is mounted at a portable frame and can be easily transported and attached to either the barrels using a flexible high-pressure and high-diameter hydraulic hose. This solution also allows for using of the USHB as a direct impact Hopkinson bar. A momentum trap is shared for both tension and compression and consists of another bar mounted to the frame using friction clamps. Residual energy is absorbed by hydro-pneumatic damper mounted at the very end of the bar system. Impact anvil attached to the input bar is used in case of tensile testing while this arrangement allows for use of small diameter pulse-shapers which is crucial to filter out unwanted high frequency oscillations from the input strain wave. The scheme of the device showing the main modular components and features of the system is shown in Figure 1. In standard configuration, the device is made up of three important components: i) a striker which generates the initial strain wave, ii) an incident bar serving as an input of the strain wave into the specimen, and iii) transmitter bar which is used for measurements of output signals behind the specimen. The mechanical properties are then determined using data from strain/velocity sensors mounted at a certain points on the bar. The device is shown in Figure 2.

2.2. ASSEMBLY AND INSTALLATION

Besides the bar system, the device consists of multiple other sub-systems such as a pneumatic launching system, electro-installation and sensors. Most of them are facilitated on the main frame which is 14 m long, allowing long pulse (impact) duration and bigger samples to be tested. The bars and the barrels used for load inducing are fastened to the main frame using specific housing. The housing of the bars is specifically designed to only allow axial movement while eliminating oscillations and ensuring proper contact during impact. To absorb the impact, a damping system is used and fastened at the end of the main frame. For tensile testing, a force transmission anvil is used to transform the impact from the striker into



FIGURE 2. Current state of the USHB.

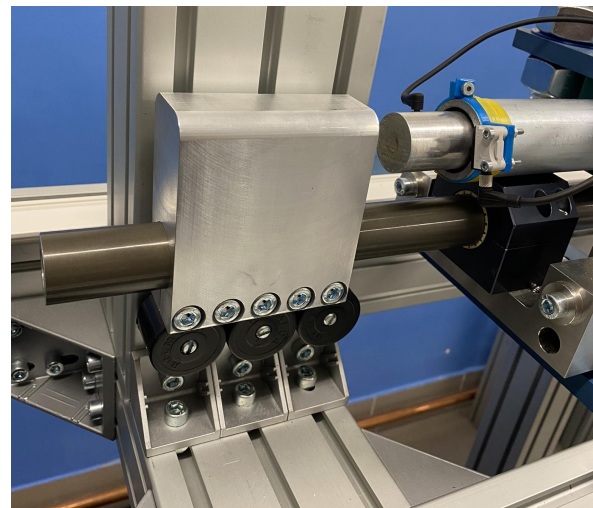


FIGURE 3. The anvil used for tensile loading.

tensile strain wave. The anvil can be seen in Figure 3.

The electro-installation represents a crucial interface and safety system providing control for some of the sensors and the pneumatic system. It is made up of electrical modules which either control the power flow, air flow in the launching system or simply indicate the current state of the device, and a switchboard containing all required circuitry. It was designed with



FIGURE 4. The pneumatic launch system.

multiple layers of safety protection such as key locks to prevent unauthorized use or state-defining light-emitting diodes (LED). All of the circuitry necessary for the operation is contained within the switchboard.

The pneumatic launching system allows the striker to be fired through air pressure and represents the most common method of striker launching first utilized by Krafft [3]. It consists of a compressor, air pressure reservoir and several electronic or manual valves. The system was designed to fulfill requirements of safe and reliable operation needing multiple valves to be in correct positions to allow for a launch. The system can be observed in Figure 4.

2.3. SENSORS

In order to record the experimental data during the experiment, the device had to be fitted with multiple sensors. The recording system uses a data acquisition module (TraNET EPC, Elsys AG, Switzerland) and signal amplifiers. Three types of sensors were used for instrumentation: i) foil strain gauges, ii) linear magnetic encoders and iii) optical gate.

Strain gauges are common element used to measure wave propagation in the bars. They detect change in resistivity which is directly proportional to strain, a fact used to capture wave shape generated during the striker's impact [14]. For experiments introduced in this paper, single pair of strain gauges was mounted at both the incident and transmission bars using adhesives. A strain gauge mounted on the bar can be seen in Figure 5

Linear magnetic encoders were used to measure displacements and velocities of the certain bar's cross-section. The sensors consist of two components, a thin magnetic strip which is attached to the bar and a readhead which is fastened to the frame using a 3D printed flange. The working principle of the sensor is mod-



FIGURE 5. Strain gauge mounted on the bar's surface.

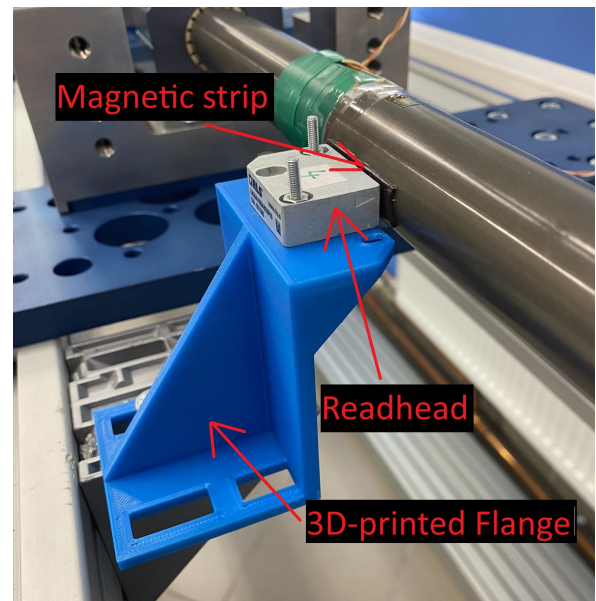


FIGURE 6. Linear magnetic encoder mounted in the vicinity of a strain gauge.

ulation of two orthogonal signals (sine and cosine) based on detection of polarity of the magnetic strip in the actual position [15]. Single sensor is mounted at each bar in the vicinity of the strain gauges to measure displacement of the bar. The encoder is featured in Figure 6.

The optical gate is a device used to detect presence of an object in an area. It is made up of two parts: an emitter and a receiver. The emitter supplies a flow of infrared light to the receiver, when it is interrupted the gate generates an electrical signal. It is placed at the barrel of the USHB and works mainly as a trigger for data recording when the beam is interrupted by a striker. The system is used as a trigger for high-speed camera(s) as well. If mounted in two positions with known distance, the sensors can be used to determine approximate striker velocity. The optical gate mounted in front of the barrel is shown in Figure 7.

Data from all the sensors are processed in the MATLAB software using a set of in-house developed functions for evaluation of Hopkinson bar experiments.

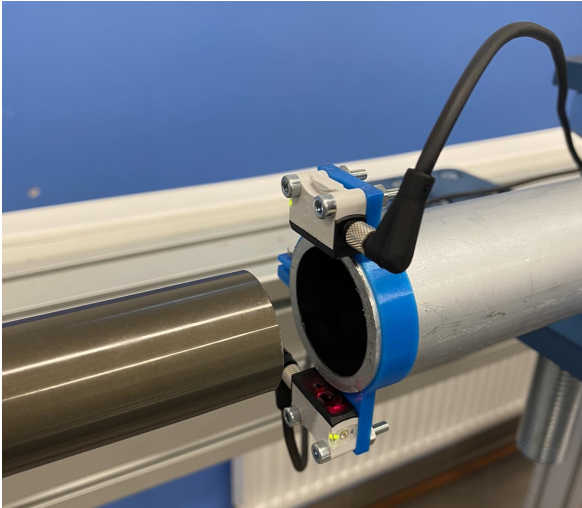


FIGURE 7. The optical gate mounted in front of a gas-gun barrel.

The measured strain signals and velocities are used for time-domain decomposition of superposed waves to prolong the standard Hopkinson bar experimental time window. The decomposition is performed using a method described in [12, 16].

2.4. CALIBRATION

Two calibration procedures were carried out to evaluate correct operation of the device and acceptable precision of the sensors, namely: force calibration and void testing.

As force is calculated using directly measured strain in the bars and known elastic properties of the bars, it is necessary to compare values indicated by strain gauges with the known force values. This is done by so called quasi-static force calibration comparing force indicated by strain gauges with a load-cell mounted in between the bars (as a specimen). The loading is performed by tightening a screw compressing both bars and the load-cell. In this paper, the calibration was done in a way to generate force from 0 to 5 kN by an increment of 500 N and then loosening it by the same amount.

Void test is in principle a split Hopkinson bar experiment without a specimen. It can be performed in two configurations – bars together and bars apart. Its purpose is to compare wave amplitudes with theoretical values and check that the elastic propagation of waves is correct. Void test can reveal bar misalignments, incorrect mounting of strain gauges, excessive friction in supports or contact problems. The device was tested with two striker lengths of 750 mm and 1500 mm out of which the longer striker represented the maximum length due to the bars' lengths being 3000 mm, twice the length of the striker bar. According to standard wave propagation theory, wavelength of the generated wave is twice as long as the striker length. If the pulse duration was longer, it would mean the input and reflected waves would interfere with each other. Both

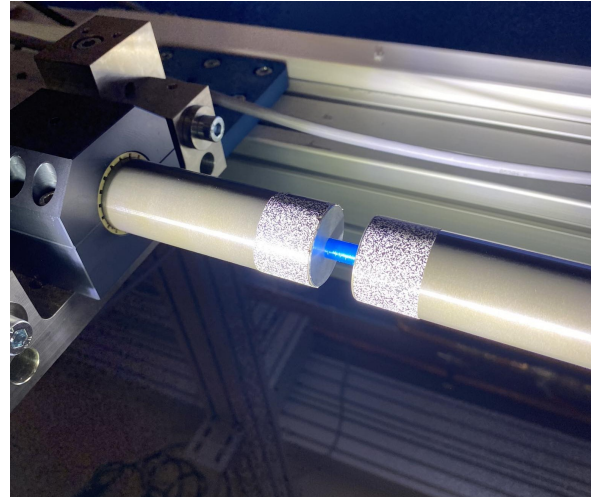


FIGURE 8. The specimen mounted in the experimental setup.

strikers were accelerated with two launching pressures of 0.5 bar and 1 bar. Six successful void tests were conducted and were also recorded by a high-speed camera.

2.5. SAMPLE TESTING

An important part in determining validity of recorded data is repeatability of tests. Due to this fact, a suitable reference sample had to be created. It was designed with a circular cross-section with a diameter of 7.5 mm and 15 mm in length. Samples were produced with 3D printing using PLA filament (Prusament PLA, Prusa, Czech Republic) with 0.2 mm layer height and 0.4 mm nozzle diameter. As an universal testing device, the USHB supports most material types while the most limiting factor constraining the experimental performance is yield strength of the bars. This particular type of specimen was selected due to its shape and production simplicity and expected forces during the impact experiment within range of the force calibration and safely below yield strength of the bars. The sample was at first subjected to a quasi-static test performed using an universal electro-mechanical testing machine. This was done to obtain referential data that could be compared to data obtained during sample testing on USHB. Two pilot tests were conducted in dynamic regime. The test conditions were the same with changing striker lengths and launching pressures as in case of the void tests. The tests were also captured using a high-speed camera with a frame-rate of 210 kfps. The specimen in the experimental setup can be viewed in Figure 8.

3. RESULTS

3.1. FORCE CALIBRATION RESULTS

The goal of the force calibration was to prove correct function of strain gauges. The results were satisfactory with the first strain gauge almost following curves recorded by the load cell, with the second strain gauge

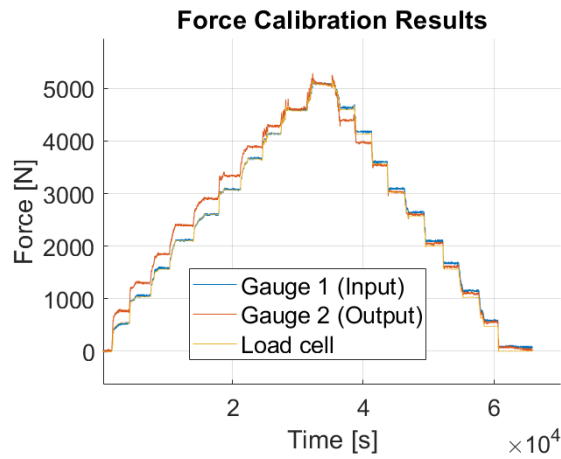


FIGURE 9. Force calibration results.

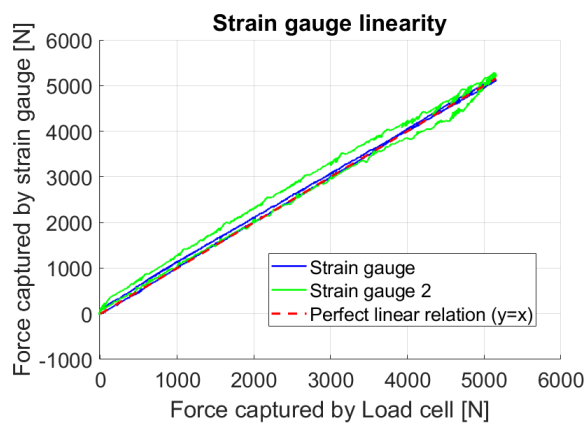


FIGURE 10. Linearity between gauge and load cell data.

however, showing some deviation, particularly at the beginning of the test. This was caused by thermal drift which is not inherently compensated in the dynamic experiments. The results could be improved by heating the gauges before calibration or adding another strain gauge disconnected from the bars. Despite this, the amplitude requirements were met with all of the sensors meeting at approx. 5 kN of force with errors for both gauges of 0.5%. The first strain gauge showed almost perfect linear behavior while the second strain gauge exhibited higher error of approximately 5% which is still acceptable for dynamic testing. The results can be viewed in Figure 9 and Figure 10.

3.2. VOID TESTS RESULTS

Void testing was meant to prove correct function of encoders and strain gauges. The main idea was to compare positional data captured by encoders, the result of which can be seen in Figure 11, with strain gauge data to analyze wave propagation according to individual striker lengths as seen in Figure 12. The result for velocity were as expected with initial amplitude of both bars reaching approximately 6.8 m s^{-1} with velocity of the output bar raised to approximately 13.5 m s^{-1} after separation of the bars. This repre-

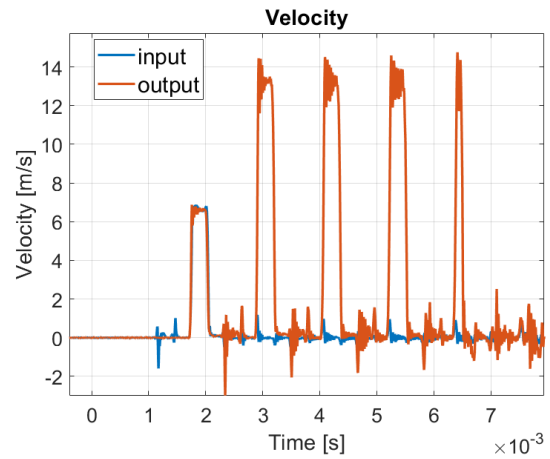


FIGURE 11. Measured velocity of both bars during a void test representing almost perfect elastic impact of two bars.

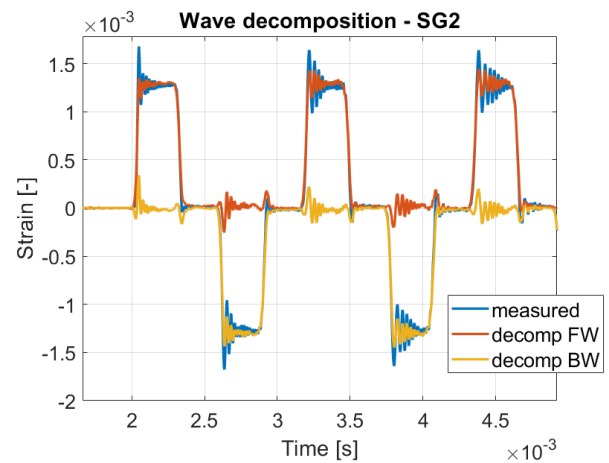


FIGURE 12. Wave decomposition from sensors of the transmission bar. As the experiment design was not to allow wave superposition of the waves, the decomposed signals should be almost identical with the measured signal.

sents almost perfect linear elastic impact of two identical bars. The velocity signals from encoders and strain signals from strain gauges were used for simple wave decomposition using elastic wave propagation theory in slender bars. If done properly with valid signals from sensors, the decomposed forward and backward propagating waves should overlap with the measured signal with respected sign (in compression forward positive and backward negative). The results for wave decomposition are shown in Figure 12 and were also up to expectations with overlapping signals and the length of pulses being in accordance with the shorter striker and came out to around $350 \mu\text{s}$.

3.3. SAMPLE TEST RESULTS

The samples were subjected to a quasi-static test with loading velocity of 1 mm min^{-1} and dynamic tests with striker impact velocity reaching 9.44 m s^{-1} and 6.55 m s^{-1} . The comparison of the results can be seen

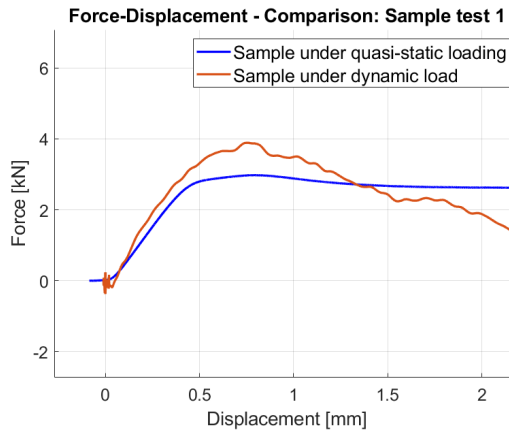


FIGURE 13. Force displacement diagrams of the first sample test – comparison of quasi-static regime and impact at 9.44 m s^{-1} .

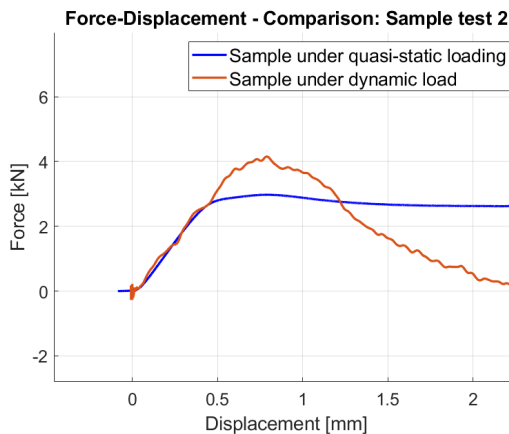


FIGURE 14. Force displacement diagrams of the second sample test – comparison of quasi-static regime and impact at 6.55 m s^{-1} .

in Figure 13 and 14. The samples were behaving differently under higher rate of deformation, showing approximately 30% increase in ultimate strength, an earlier collapse and failure than during quasi-static deformation, which is expected for this type of material and testing. The specimen deforming during dynamic compression is shown in 15.

3.4. TENSILE TESTING

Tensile test is technically different from a compression experiment as the sample must be fastened to both bars and tensile waves have to propagate through it. Pilot tensile experiments were conducted, however problems with insufficient strain waves quality were observed. Insufficient rigidity of the supports of the tensile anvil was determined as a cause and will require strengthening of this component. Due to stress being imposed asymmetrically during the force transfer through the anvil, a certain amount of distortion of the signal is to be expected. This might seem to render the anvil solution obsolete since in SPH designs made especially for dynamic tensile testing the use of tubular impactors, as featured, for

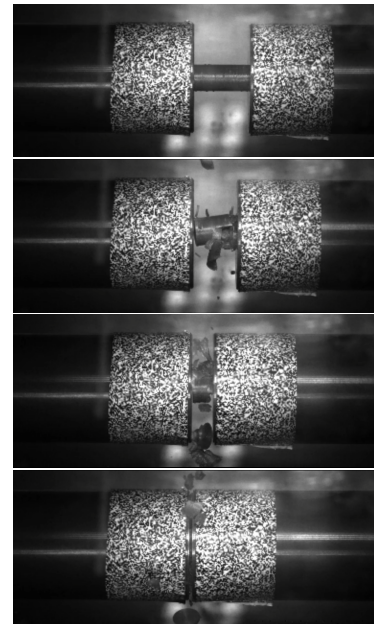


FIGURE 15. A slideshow showing collapse of the specimen in compression – experiment duration 9 ms.

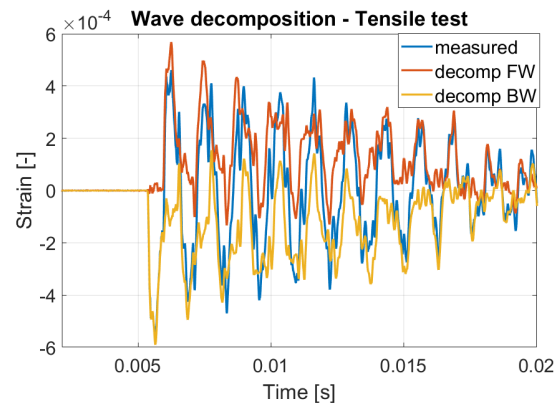


FIGURE 16. Waves recorded during a tensile void test and results of the wave decomposition.

example, in [17], has become a norm due to its capability to stress the incidental bar symmetrically. This setup, however, is technologically far more complex and costly. Therefore the anvil solution was used despite its disadvantages. Still, the waves were successfully recorded and even the wave decomposition could be calculated from the data revealing parasitic bending of the input bar. The strain waves and results of the decomposition are shown in Figure 16.

4. CONCLUSIONS

USHB with modular design allowing for easy rearrangement to different experimental variants was successfully assembled and commissioned. The device was instrumented with strain gauges and linear magnetic encoders for measurement of strain waves, displacements and velocities during the experiments. Calibration procedures were successfully conducted in quasi-static regime to check correct mounting, align-

ment, sensitivity of strain gauges, and validity of the indicated force. Dynamic calibration was performed by series of void tests to check correct function of strain gauges, linear encoders, experiment triggering, and suitability of signals for subsequent wave decomposition. All the tests produced satisfactory results. Pilot testing in uni-axial compression were performed with cylindrical specimens produced by 3D printing while the results were compared with quasi-static compression in standard testing device. The evaluated results were comparable with the quasi-static data while positive strain rate sensitivity with significant weakening of the specimen and its rupture at lower strain were observed. Although problems with parasitic bending of the impact anvil were present during the tests in tensile arrangement, the strain waves were validly measured and the setup was considered suitable for testing of the specimens in tension after (currently ongoing) strengthening of the anvil support.

ACKNOWLEDGEMENTS

The research was supported by the Czech Science Foundation (project Junior Star no. 22-18033M).

REFERENCES

- [1] H. Kolsky. An investigation of the mechanical properties of materials at very high rates of strain. *Proceedings of the Physical Society Section B* **62**(11):676–700, 1949. <https://doi.org/10.1088/0370-1301/62/11/302>
- [2] R. M. Davies. A critical study of the Hopkinson pressure bar. *Philosophical Transactions of the Royal Society of London Series A, Mathematical and Physical Sciences* **240**(821):375–457, 1948. <https://doi.org/10.1098/rsta.1948.0001>
- [3] J. M. Krafft, A. M. Sullivan, C. F. Tipper. The effect of static and dynamic loading and temperatures on the yield stress of iron and mild steel in compression. *Proceedings of the Royal Society A* **221**(1144), 1954. <https://doi.org/10.1098/rspa.1954.0009>
- [4] P. Verleysen. Shear testing using the Kolsky-Hopkinson bar machine. In R. Othman (ed.), *The Kolsky-Hopkinson Bar Machine: Selected Topics*, pp. 75–120. Springer International Publishing, Cham, 2018. https://doi.org/10.1007/978-3-319-71919-1_3
- [5] L. Corallo, G. Mirone, P. Verleysen. A novel high-speed bulge test to identify the large deformation behavior of sheet metals. *Experimental Mechanics* **63**:593–607, 2023. <https://doi.org/10.1007/s11340-022-00936-5>
- [6] Y. Chen, K. Liu, Z. Xu, et al. A comprehensive experimental investigation of the rate-dependent interlaminar delamination behaviour of CFRP composites. *Composites Part B: Engineering* **261**:110788, 2023. <https://doi.org/10.1016/j.compositesb.2023.110788>
- [7] L. Le Barbenchon, M. Lißner. On the dynamic performance of additively manufactured visco-elastic meta-materials. *Materials Letters* **359**:135823, 2024. <https://doi.org/10.1016/j.matlet.2023.135823>
- [8] R. Govender, R. Curry. The “Open” Hopkinson Pressure Bar: Towards addressing force equilibrium in specimens with non-uniform deformation. *Journal of Dynamic Behavior of Materials* **2**:43–49, 2015. <https://doi.org/10.1007/s40870-015-0042-2>
- [9] P. Jakkula, G. Ganzenmüller, S. Hiermaier. A Direct Impact Tension Bar setup for testing low-impedance materials at intermediate rates of strain. *Materials Letters* **352**:135082, 2023. <https://doi.org/10.1016/j.matlet.2023.135082>
- [10] P. Jakkula, A. Cohen, B. Lukić, et al. Split Hopkinson Tension Bar and Universal Testing Machine for high-speed X-ray imaging of materials under tension. *Instruments* **6**(3):38, 2022. <https://doi.org/10.3390/instruments6030038>
- [11] S. Kim, D. G. Kim, M. Kim, et al. Analyses of impact energy-absorbing performance of open- and closed-cell Al foams using modified split Hopkinson pressure bar. *Journal of Alloys and Compounds* **965**:171349, 2023. <https://doi.org/10.1016/j.jallcom.2023.171349>
- [12] T. Fíla, P. Koudelka, J. Falta, et al. Dynamic impact testing of cellular solids and lattice structures: Application of two-sided direct impact Hopkinson bar. *International Journal of Impact Engineering* **148**:103767, 2021. <https://doi.org/10.1016/j.ijimpeng.2020.103767>
- [13] T. Fíla, J. Falta, P. Koudelka, et al. Flash X-ray radiography of internal damage in soft cellular materials during instrumented dynamic penetration. *Materials Letters* **354**:135372, 2024. <https://doi.org/10.1016/j.matlet.2023.135372>
- [14] K. Hoffmann. *An introduction to measurements using strain gages*. Hottinger Baldwin Messtechnik GmbH, Darmstadt, 1989.
- [15] J. Gao. Dynamic penetration of cellular solids: Experimental investigation using Hopkinson bar and computed tomography. *Materials Science and Engineering: A* **800**:140096, 2021. <https://doi.org/10.1016/j.msea.2020.140096>
- [16] L. Leicht, T. Fíla, P. Máca, M. Curbach. Dynamic beam-end tests: Investigation using split Hopkinson bar. *International Journal of Impact Engineering* **172**:104417, 2023. <https://doi.org/10.1016/j.ijimpeng.2022.104417>
- [17] R. Gerlach, C. Kettenbeil, N. Petrinic. A new split Hopkinson tensile bar design. *International Journal of Impact Engineering* **50**:63–67, 2012. <https://doi.org/10.1016/j.ijimpeng.2012.08.004>